Journal of Physics: Conference Series **316** (2011) 012018 doi:10.1088/1742-6596/316/1/012018

Jet Physics in pp and PbPb Collisions with the CMS Experiment

Edward Wenger, for the CMS Collaboration [1]

Massachusetts Institute of Technology, Cambridge, Massachusetts, United States

E-mail: edwenger@mit.edu

Abstract. The properties of dijets are reviewed for pp and PbPb collisions recorded by the CMS experiment. In particular, a dramatic quenching of jets is observed as a significant imbalance in the transverse momenta of dijets in central PbPb collisions at a center-of-mass energy of 2.76 TeV. The redistribution of the quenched jet energy is studied using the transverse momentum balance of charged tracks projected onto the direction of the leading jet. In contrast to pp collisions, a large fraction of the momentum balance for asymmetric jets is carried by low momentum particles at large angular distance to the jet axis.

1. Introduction

Fully-reconstructed dijets are a powerful tool for tomographically probing the hot, dense medium produced in ultra-relativistic collisions of heavy ions. By quantifying the pattern of partonic energy loss and the redistribution of energy in the medium, one can access experimentally the properties of the medium, e.g., the gluon density (dN_g/dy) or the transport coefficient ($\hat{q}$).

The energy-loss mechanism has been studied already at RHIC in a more indirect fashion, namely measurements of two-particle angular correlations between charged particles. For charged particles with moderate transverse momentum ($p_{\mathrm{T}}^{\mathrm{trig}} = 4$–$6\,\mathrm{GeV}/c$, $p_{\mathrm{T}}^{\mathrm{assoc}} = 2$–$4\,\mathrm{GeV}/c$), the characteristic away-side jet correlation that is prominent in pp collisions is nearly extinguished in central PbPb collisions [1]. While this observation represents strong indirect evidence of jet quenching at RHIC, direct jet reconstruction [2, 3] — especially of the most strongly quenched dijets — is challenging due to fluctuations in the soft underlying event.

At $\sqrt{s_{\mathrm{NN}}} = 2.76\,\mathrm{TeV}$, copious production of high-E_{T} jets above $100\,\mathrm{GeV}$ gives a much larger separation between the hard and soft scales. Even looking at event displays in the first days of the 2010 PbPb run, a significant imbalance was apparent in reconstructed dijets [4, 5]. For the first time, it is possible to reconstruct strongly modified dijets unambiguously above the soft background (see Fig. 1), marking the beginning of a new era of more powerful studies of jet quenching at the LHC.

2. Analysis Methods

The dijet analysis presented in these proceedings was performed using the data collected in 2010 from PbPb collisions at a nucleon-nucleon center-of-mass energy of $\sqrt{s_{\mathrm{NN}}} = 2.76\,\mathrm{TeV}$ at

[1] The complete CMS collaboration is listed in a recent submission to *Phys. Rev. C* [4], from which the text of these proceedings is largely excerpted.

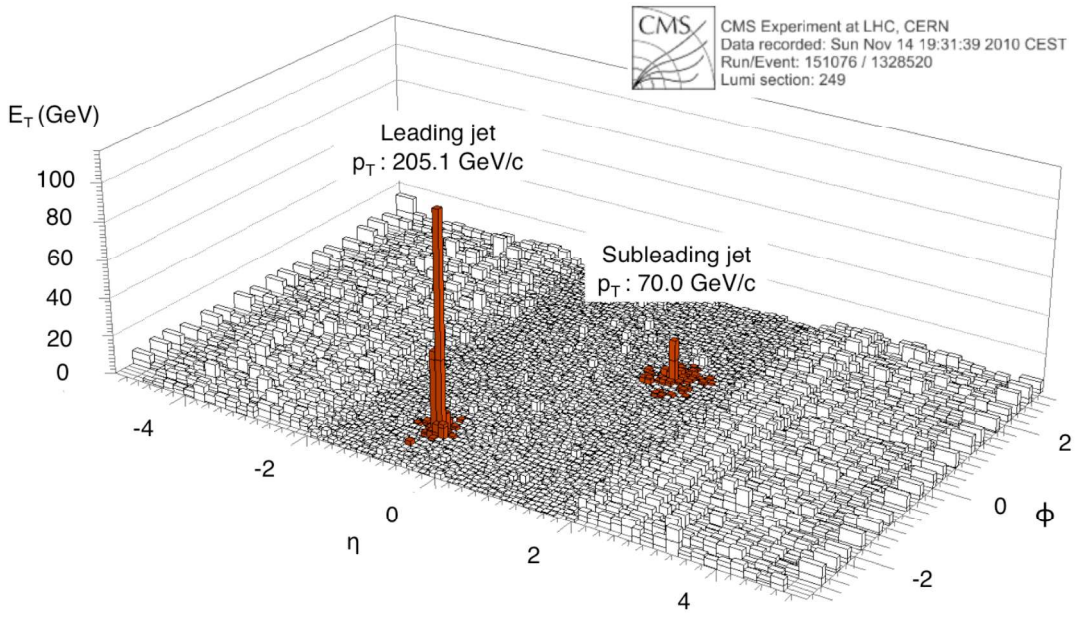

Figure 1. Example of an unbalanced dijet in a PbPb collision event at $\sqrt{s_{\mathrm{NN}}} = 2.76\,\mathrm{TeV}$. Plotted is the summed transverse energy in the electromagnetic and hadron calorimeters vs. η and ϕ, with the identified jets highlighted in red, and labeled with the corrected jet transverse momentum.

the Compact Muon Solenoid (CMS) detector. The data included in this measurement correspond to a total integrated luminosity of $6.7\,\mu\mathrm{b}^{-1}$.

Jets are identified primarily using the energy deposited in the lead-tungstate crystal electromagnetic calorimeter (ECAL) and the brass/scintillator hadron calorimeter (HCAL) covering $|\eta| < 3$. In addition, a steel/quartz-fiber Cherenkov calorimeter, called Hadron Forward (HF), covers the forward rapidities $3 < |\eta| < 5.2$ and is used to determine the centrality of the PbPb collision. The central calorimeters are embedded in a solenoid with 3.8 T central magnetic field. The CMS tracking system, located inside the calorimeter, consists of pixel and silicon-strip layers covering $|\eta| < 2.5$, and provides track reconstruction down to $p_{\mathrm{T}} \approx 100\,\mathrm{MeV}/c$, with a track momentum resolution of about 1% at $p_{\mathrm{T}} = 100\,\mathrm{GeV}/c$. A set of scintillator tiles, the Beam Scintillator Counters (BSC), are mounted on the inner side of the HF calorimeters for triggering and beam-halo rejection. The full details of the CMS detector are described in Ref. [6].

For online event selection, CMS uses a two-level trigger system: Level-1 (L1) and High Level Trigger (HLT). The events for this analysis were selected using an inclusive single-jet trigger that required an L1 jet with $p_{\mathrm{T}} > 30\,\mathrm{GeV}/c$ and an HLT jet with $p_{\mathrm{T}} > 50\,\mathrm{GeV}/c$, where neither p_{T} value was corrected for the p_{T}-dependent calorimeter energy response. The trigger becomes fully efficient for collisions with a leading jet with corrected p_{T} greater than $100\,\mathrm{GeV}/c$.

For the analysis of PbPb events, it is important to know the "centrality" of the collision, i.e., whether the overlap of the two colliding nuclei is large or small. In this analysis, the total energy deposited in both HF calorimeters was used to divide the event sample into five centrality classes, corresponding to the most central 10% of the events, the next most central 10% of the events (denoted 10–20%), and further bins corresponding to the 20–30%, 30–50%, and 50–100% selections of the total hadronic cross section.

The baseline jet reconstruction for heavy ion collisions in CMS is performed with an iterative cone algorithm modified to subtract the soft underlying event on an event-by-event basis [7].

Each cone is selected with a radius $\Delta R = \sqrt{\Delta\phi^2 + \Delta\eta^2} = 0.5$ around a seed of minimum transverse energy of 1 GeV. The performance of this algorithm is documented in Ref. [4]. Jet corrections for the calorimeter response have been applied, as determined in studies for pp collisions [8]. When applying the algorithm to PbPb data, the subtracted background energy for $R = 0.5$ jet cones ranges from 6–13 GeV for peripheral events (centrality bins 50–100%) to 90–130 GeV for central collisions (0–10%), before applying jet energy scale corrections.

The basic offline selection of events for the dijet analysis is the presence of a leading calorimeter jet in the pseudorapidity range of $|\eta| < 2$ with a corrected jet $p_{\mathrm{T}} > 120\,\mathrm{GeV}/c$. By selecting these leading jets we avoid possible biases due to inefficiencies close to the trigger threshold. Furthermore, the selection of a rather large leading jet momentum expands the range of jet momentum imbalances that can be observed between the leading and subleading jets, as the subleading jets need a minimum momentum of $p_{\mathrm{T}} > 35$–$50\,\mathrm{GeV}/c$ to be reliably detected above the high-multiplicity underlying event in PbPb collisions. In order to ensure a high quality dijet selection, additional kinematic selection cuts were applied. The azimuthal angle between the leading and subleading jets was required to be at least $2\pi/3$. A minimum p_{T} of $p_{\mathrm{T},1} > 120\,\mathrm{GeV}/c$ was required for leading jets and $p_{\mathrm{T},2} > 50\,\mathrm{GeV}/c$ for subleading jets. No explicit requirement is made either on the presence or absence of a third jet in the event.

For the analysis of dijet properties in PbPb events, it is crucial to understand how the jet reconstruction is modified in the presence of the high multiplicity of particles produced in the PbPb underlying event. The jet-finding performance was studied using dijets in pp collisions simulated with the PYTHIA event generator (version 6.423, tune D6T) [9], modified for the isospin content of the colliding nuclei [10]. In order to enhance the number of Pythia dijets in the momentum range studied, a minimum $\hat{p}_{\mathrm{T}}$ selection of $80\,\mathrm{GeV}/c$ was used. Lower $\hat{p}_{\mathrm{T}}$ selections, as discussed in [11], were also investigated and found to agree with the $\hat{p}_{\mathrm{T}} = 80\,\mathrm{GeV}/c$ results within uncertainties. The PYTHIA dijet events were processed with the full detector simulation and analysis chain. Additional samples were produced in which the PYTHIA dijet events were embedded into a minimum bias selection of PbPb events at the raw data level. For this embedding procedure, both real PbPb data events (PYTHIA+DATA), and PbPb events simulated with the HYDJET event generator [10] (PYTHIA+HYDJET) were used. The HYDJET parameters were tuned to reproduce the total particle multiplicities at all centralities and to approximate the underlying event fluctuations seen in data. The HYDJET events included the simulation of hard-scattering processes for which radiative parton energy loss was simulated, but collisional energy loss was turned off [10]. Both embedded samples were propagated through the standard reconstruction and analysis chain.

3. Calorimeter Jet Imbalance

The goal of this analysis is to characterize possible modifications of dijet properties as a function of centrality in PbPb collisions. One possible medium effect on the dijet properties is a change of the back-to-back alignment of the two partons. This can be studied using the event-normalized differential dijet distribution, $(1/N)(dN/d\Delta\phi_{12})$, versus $\Delta\phi_{12}$. Figure 2 shows distributions of $\Delta\phi_{12}$ between leading and subleading jets which pass the respective p_{T} selections. In Fig. 2 (a), the dijet $\Delta\phi_{12}$ distributions are plotted for 7 TeV pp data in comparison to the corresponding PYTHIA simulations using the anti-k_{T} algorithm for jets based on calorimeter information. PYTHIA provides a good description of the experimental data, with slightly larger tails seen in the PYTHIA simulations. It is important to note that the PYTHIA simulations include events with more than two jets, which provide the main contribution to events with large momentum imbalance or $\Delta\phi_{12}$ far from π.

Figures 2 (b)–(f) show the dijet $\Delta\phi_{12}$ distributions for PbPb data in five centrality bins, compared to PYTHIA+DATA simulations. The distributions for the four more peripheral bins are in good agreement with the PYTHIA+DATA reference, especially for $\Delta\phi_{12} \gtrsim 2$. The three

centrality bins spanning 0–30% show an excess of events with azimuthally misaligned dijets ($\Delta\phi_{12} \lesssim 2$), compared with more peripheral events. A similar trend is seen for the PYTHIA+DATA simulations, although the fraction of events with azimuthally misaligned dijets is smaller in the simulation. The centrality dependence of the azimuthal correlation in PYTHIA+DATA can be understood as the result of the increasing fake-jet rate and the drop in jet reconstruction efficiency near the 50 GeV/c threshold from 95% for peripheral events to 88% for the most central events. In PbPb data, this effect is magnified since low-p_{T} away-side jets can undergo a sufficiently large energy loss to fall below the 50 GeV/c selection criteria.

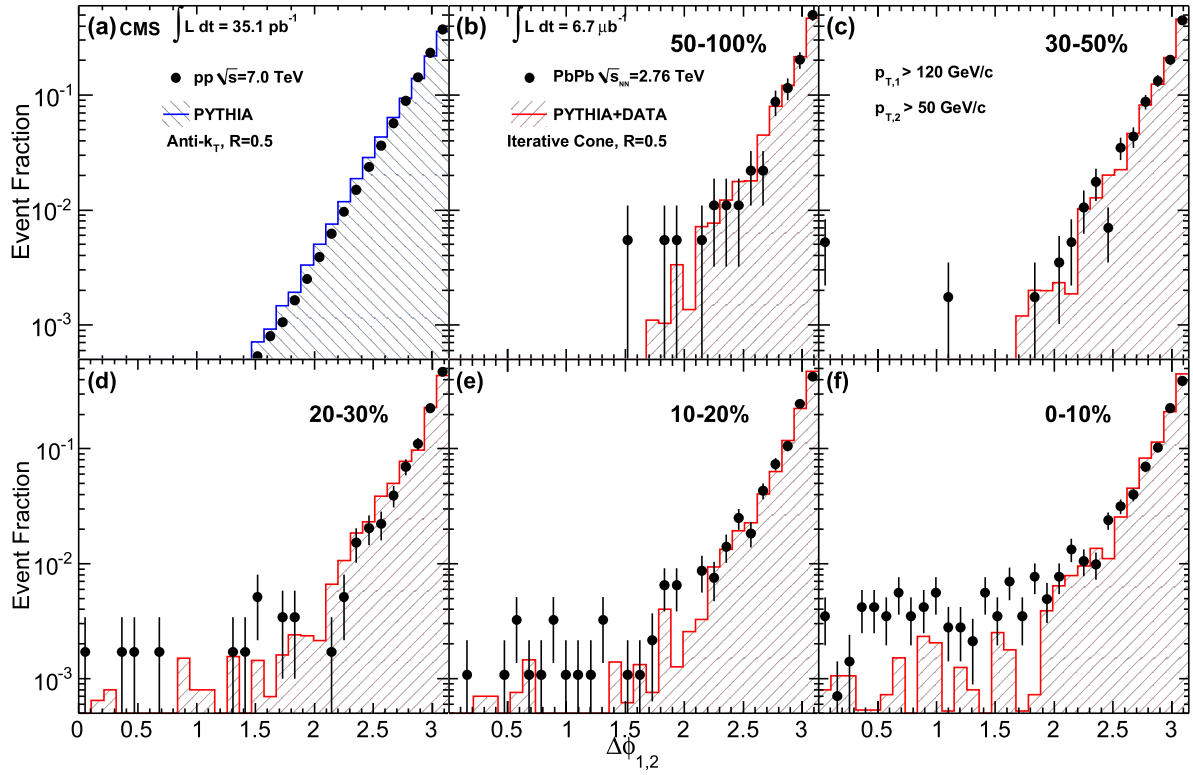

Figure 2. $\Delta\phi_{12}$ distributions for leading jets of $p_{\mathrm{T},1} > 120$ GeV/c with subleading jets of $p_{\mathrm{T},2} > 50$ GeV/c for 7 TeV pp collisions (a) and 2.76 TeV PbPb collisions in several centrality bins: (b) 50–100%, (c) 30–50%, (d) 20–30%, (e) 10–20% and (f) 0–10%. Data are shown as black points, while the histograms show (a) PYTHIA events and (b)-(f) PYTHIA events embedded into PbPb data. The error bars show the statistical uncertainties.

To characterize the dijet momentum balance (or imbalance) quantitatively, we use the asymmetry ratio,

$$A_J = \frac{p_{\mathrm{T},1} - p_{\mathrm{T},2}}{p_{\mathrm{T},1} + p_{\mathrm{T},2}} \ , \tag{1}$$

where the subscript 1 always refers to the leading jet, so that A_J is positive by construction. The use of A_J removes uncertainties due to possible shifts in the overall normalization of the jet energy scale. It is important to note that the subleading jet $p_{\mathrm{T},2} > 50$ GeV/c selection imposes a $p_{\mathrm{T},1}$-dependent limit on the magnitude of A_J. For example, for the most frequent leading jets near the 120 GeV/c threshold, this limit is $A_J < 0.41$, while the largest possible A_J for the

present dataset is 0.7 for 300 GeV/c leading jets. Dijets in which the subleading jet is lost below the 50 GeV/c threshold are not included in the A_J calculation.

In Fig. 3 (a), the A_J dijet asymmetry observable calculated by PYTHIA is compared to pp data at $\sqrt{s} = 7$ TeV. Again, data and event generator are found to be in excellent agreement. This observation, as well as the good agreement between PYTHIA+DATA and the most peripheral PbPb data shown in Fig. 3 (b), suggests that PYTHIA at $\sqrt{s} = 2.76$ TeV can serve as a good reference for the dijet imbalance analysis in PbPb collisions.

The centrality dependence of A_J for PbPb collisions can be seen in Figs. 3 (b)–(f), in comparison to PYTHIA+DATA simulations. Whereas the dijet angular correlations show only a small dependence on collision centrality, the dijet momentum balance exhibits a dramatic change in shape for the most central collisions. In contrast, the PYTHIA simulations only exhibit a modest broadening, even when embedded in the highest multiplicity PbPb events.

Central PbPb events show a significant deficit of events in which the momenta of leading and subleading jets are balanced and a significant excess of unbalanced pairs. The large excess of unbalanced compared to balanced dijets explains why this effect was apparent even when simply scanning event displays (see Fig. 1). The striking momentum imbalance is also confirmed when studying high-p_{T} tracks associated with leading and subleading jets, as will be shown in Section 4. It is consistent with a degradation of the parton energy, or jet quenching, in the medium produced in central PbPb collisions.

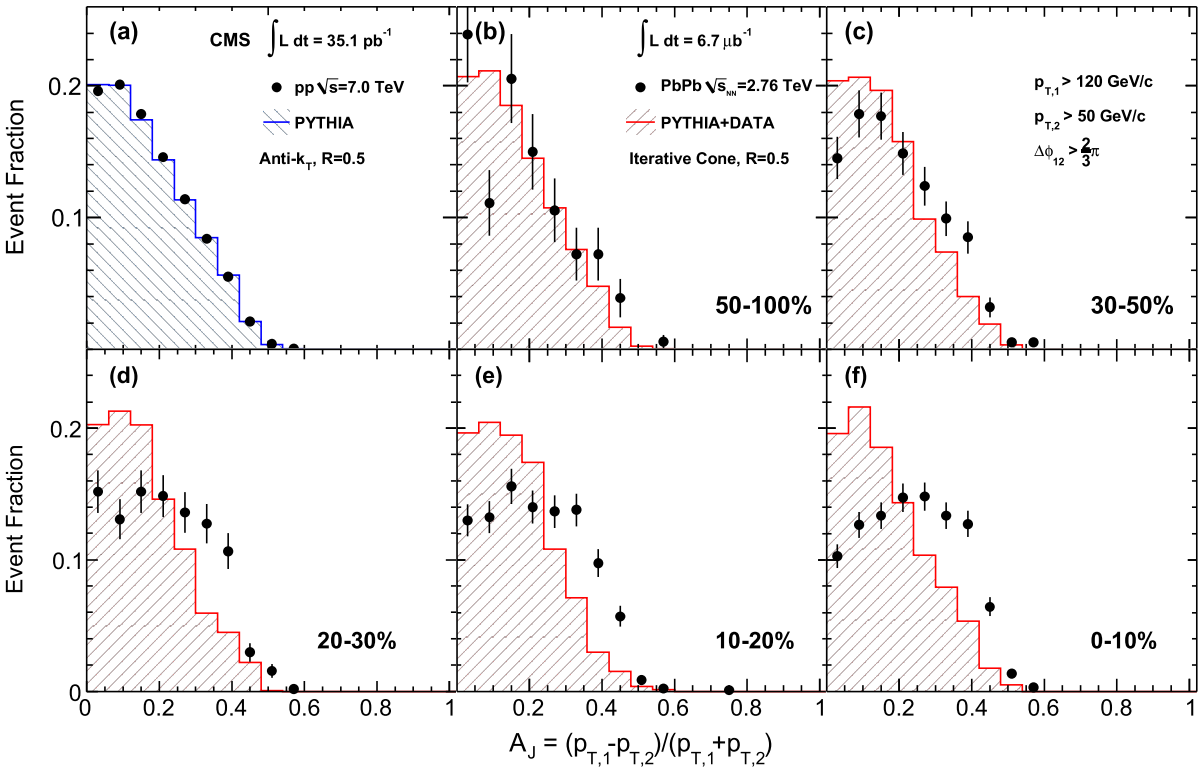

Figure 3. Dijet asymmetry ratio, A_J, for leading jets of $p_{\mathrm{T},1} > 120$ GeV/c, subleading jets of $p_{\mathrm{T},2} > 50$ GeV/c, and $\Delta\phi_{12} > 2\pi/3$ for 7 TeV pp collisions (a) and 2.76 TeV PbPb collisions in several centrality bins: (b) 50–100%, (c) 30–50%, (d) 20–30%, (e) 10–20% and (f) 0–10%. Data are shown as black points, while the histograms show (a) PYTHIA events and (b)-(f) PYTHIA events embedded into PbPb data. The error bars show the statistical uncertainties.

4. Energy Balance in Charged Tracks

The studies of calorimeter jets show a strong change of the jet momentum balance as a function of collision centrality. This implies a corresponding modification in the distribution of jet fragmentation products, with energy being either transported out of the cone area used to define the jets, or to low-momentum particles that are not measured in the calorimeter jets. By using the information from reconstructed charged particles in the tracker, we have an opportunity to do the first in-depth studies of where the missing energy is redistributed, whether to low-momentum particles or to large angles from the jet axis.

The study of the overall momentum balance in the dijet events is performed using the projection of missing p_{T} of reconstructed charged tracks onto the leading jet axis. For each event, this projection is calculated as

$$\not{p}_{\mathrm{T}}^{\parallel} = \sum_{\mathrm{i}} -p_{\mathrm{T}}^{\mathrm{i}} \cos\left(\phi_{\mathrm{i}} - \phi_{\text{Leading Jet}}\right), \tag{2}$$

where the sum is over all tracks with $p_{\mathrm{T}} > 0.5\,\mathrm{GeV}/c$ and $|\eta| < 2.4$. The results are then averaged over events to obtain $\langle \not{p}_{\mathrm{T}}^{\parallel} \rangle$.

In Fig. 4, $\langle \not{p}_{\mathrm{T}}^{\parallel} \rangle$ is shown as a function of A_J for two centrality bins, 30–100% (left) and 0–30% (right). Results for PYTHIA+HYDJET are presented in the top row, while the bottom row shows the results for PbPb data. Using tracks with $|\eta| < 2.4$ and $p_{\mathrm{T}} > 0.5\,\mathrm{GeV}/c$, one sees that indeed the momentum balance of the events, shown as solid circles, is recovered within uncertainties, for both centrality ranges and even for events with large observed dijet asymmetry, in both data and simulation. This shows that the dijet momentum imbalance is not related to undetected activity in the event due to instrumental (e.g. gaps or inefficiencies in the calorimeter).

The figure also shows the contributions to $\langle \not{p}_{\mathrm{T}}^{\parallel} \rangle$ for five transverse momentum ranges from 0.5–1 GeV/c to $p_{\mathrm{T}} > 8\,\mathrm{GeV}/c$. The vertical bars for each range denote statistical uncertainties. For data and simulation, a large negative contribution to $\langle \not{p}_{\mathrm{T}}^{\parallel} \rangle$ (i.e., in the direction of the leading jet) by the $p_{\mathrm{T}} > 8\,\mathrm{GeV}/c$ range is balanced by the combined contributions from the 0.5–8 GeV/c regions. Looking at the $p_{\mathrm{T}} < 8\,\mathrm{GeV}/c$ region in detail, important differences between data and simulation emerge. For PYTHIA+HYDJET both centrality ranges show a large balancing contribution from the intermediate p_{T} region of 4–8 GeV/c, while the contribution from the two regions spanning 0.5–2 GeV/c is very small. In peripheral PbPb data, the contribution of 0.5–2 GeV/c tracks relative to that from 4–8 GeV/c tracks is somewhat enhanced compared to the simulation. In central PbPb events, the relative contribution of low and intermediate-p_{T} tracks is actually the opposite of that seen in PYTHIA+HYDJET. In data, the 4–8 GeV/c region makes almost no contribution to the overall momentum balance, while a large fraction of the negative imbalance from high p_{T} is recovered in low-momentum tracks.

Further insight into the radial dependence of the momentum balance can be gained by studying $\langle \not{p}_{\mathrm{T}}^{\parallel} \rangle$ separately for tracks inside cones of size $\Delta R = 0.8$ around the leading and subleading jet axes, and for tracks outside of these cones. The results of this study for central events are shown in Fig. 5 for the in-cone balance and out-of-cone balance for MC and data. As the underlying PbPb event in both data and MC is not ϕ-symmetric on an event-by-event basis, the back-to-back requirement was tightened to $\Delta\phi_{12} > 5\pi/6$ for this study.

One observes that for both data and MC an in-cone imbalance of $\langle \not{p}_{\mathrm{T}}^{\parallel} \rangle \approx -20\,\mathrm{GeV}/c$ is found for the $A_J > 0.33$ selection. In both cases this is balanced by a corresponding out-of-cone imbalance. However, in the PbPb data the out-of-cone contribution is carried almost entirely by tracks with $0.5 < p_{\mathrm{T}} < 4\,\mathrm{GeV}/c$, whereas in MC more than 50% of the balance is carried by tracks with $p_{\mathrm{T}} > 4\,\mathrm{GeV}/c$, with a negligible contribution from $p_{\mathrm{T}} < 1\,\mathrm{GeV}/c$. The PYTHIA+HYDJET results are indicative of semi-hard initial or final-state radiation as the underlying cause for large A_J events in the MC study. This has been confirmed by further studies which showed that in

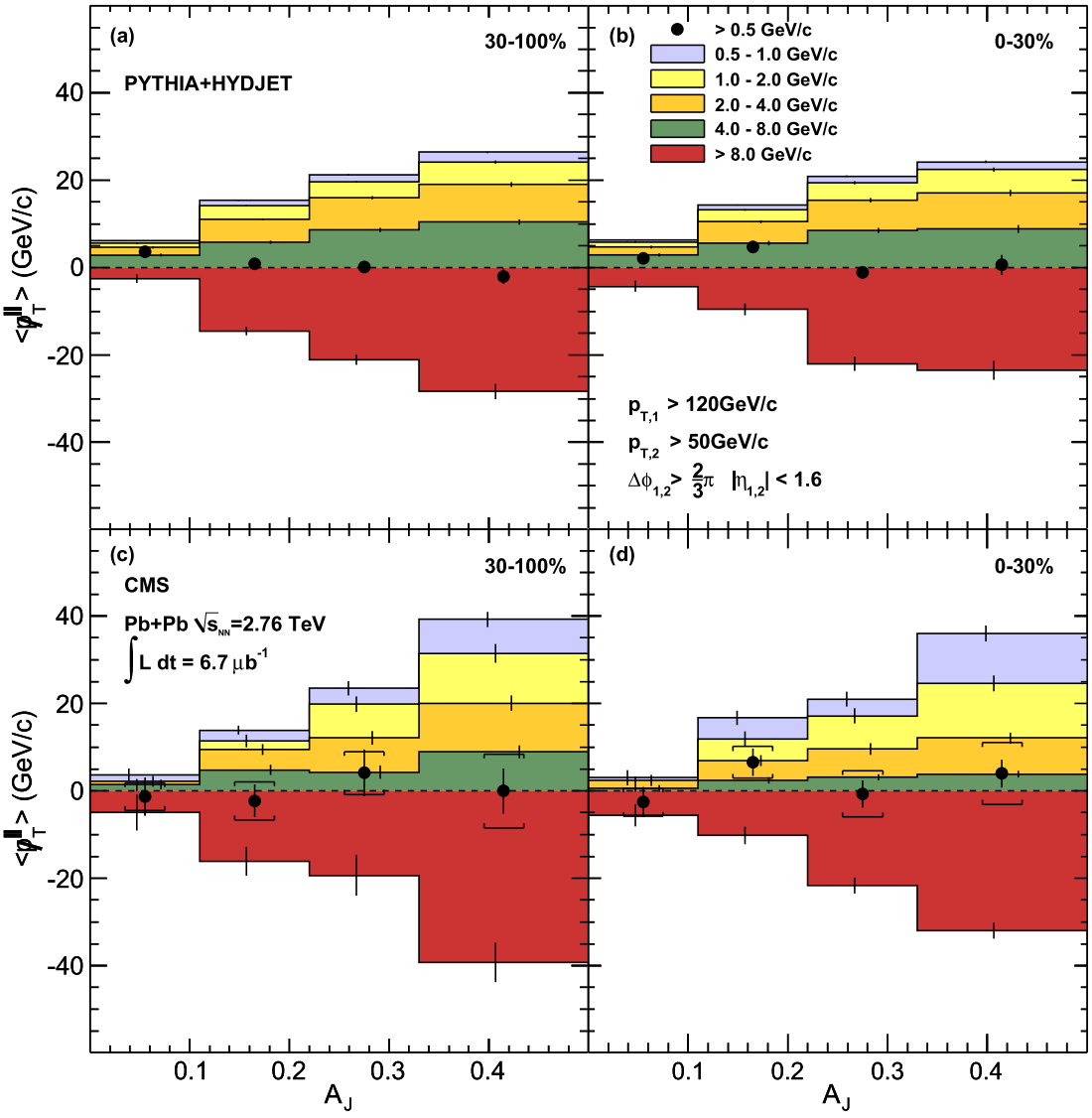

Figure 4. Average missing transverse momentum, $\langle p_{\mathrm{T}}^{\parallel} \rangle$, for tracks with $p_{\mathrm{T}} > 0.5\,\mathrm{GeV}/c$, projected onto the leading jet axis (solid circles). The $\langle p_{\mathrm{T}}^{\parallel} \rangle$ values are shown as a function of dijet asymmetry A_J for 30–100% centrality (left) and 0–30% centrality (right). For the solid circles, vertical bars and brackets represent the statistical and systematic uncertainties, respectively. Colored bands show the contribution to $\langle p_{\mathrm{T}}^{\parallel} \rangle$ for five ranges of track p_{T}. The top and bottom rows show results for PYTHIA+HYDJET and PbPb data, respectively. For the individual p_{T} ranges, the statistical uncertainties are shown as vertical bars.

PYTHIA the momentum balance in the transverse plane for events with large A_J can be restored if a third jet with $p_{\mathrm{T}} > 20\,\mathrm{GeV}/c$, which is present in more than 90% of these events, is included. This is in contrast to the results for large-A_J PbPb data, which show that a large part of the momentum balance is carried by soft particles ($p_{\mathrm{T}} < 2\,\mathrm{GeV}/c$) and radiated at large angles to the jet axes ($\Delta R > 0.8$).

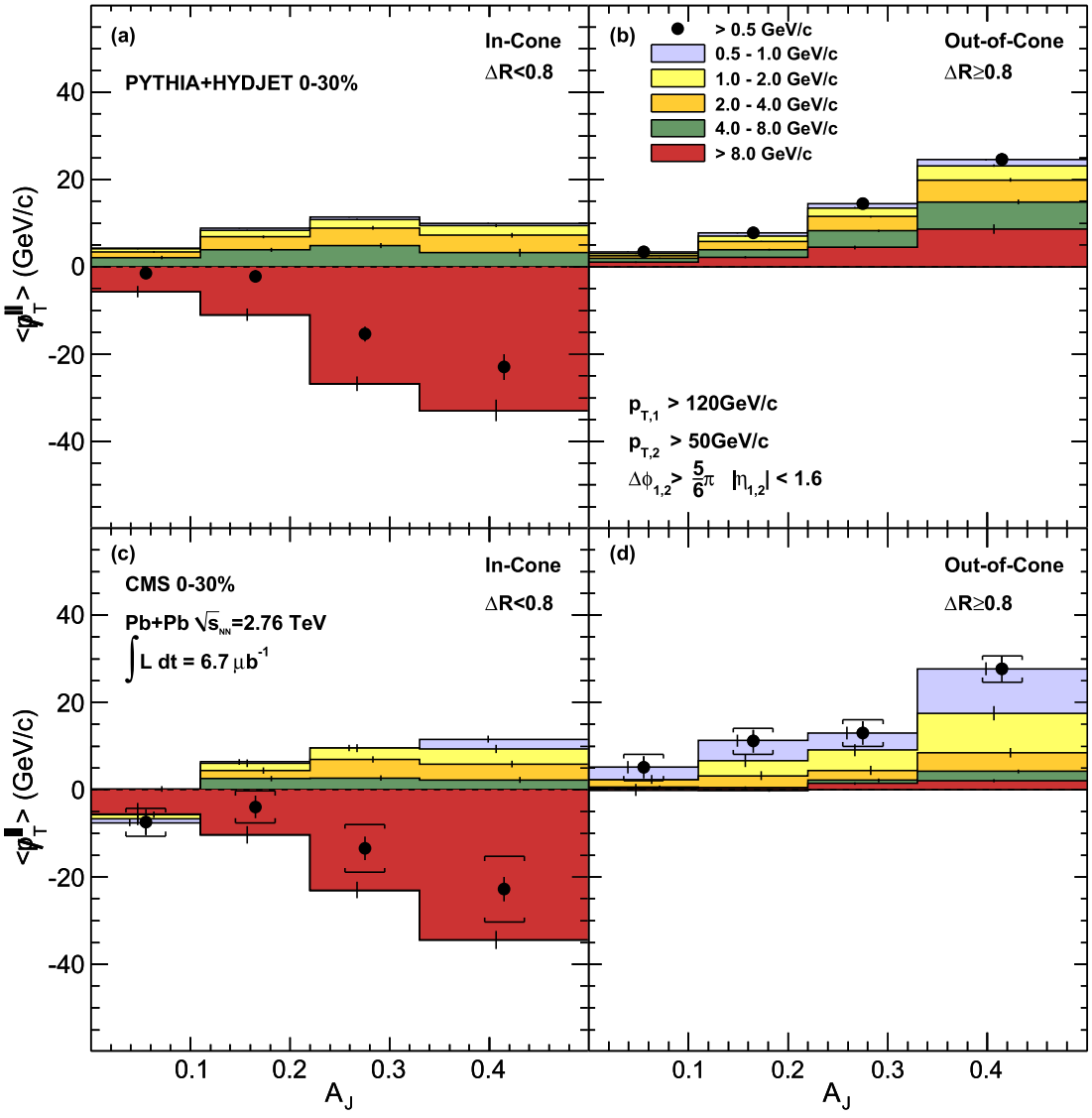

Figure 5. Average missing transverse momentum, $\langle p_{\mathrm{T}}^{\parallel} \rangle$, for tracks with $p_{\mathrm{T}} > 0.5\,\mathrm{GeV}/c$, projected onto the leading jet axis (solid circles). The $\langle p_{\mathrm{T}}^{\parallel} \rangle$ values are shown as a function of dijet asymmetry A_J for 0–30% centrality, inside ($\Delta R < 0.8$) one of the leading or subleading jet cones (left) and outside ($\Delta R > 0.8$) the leading and subleading jet cones (right). For the solid circles, vertical bars and brackets represent the statistical and systematic uncertainties, respectively. For the individual p_{T} ranges, the statistical uncertainties are shown as vertical bars.

5. Summary

The properties of dijets have been measured in pp and PbPb collisions recorded by the CMS experiment. A significant imbalance in the transverse momenta of dijets is observed in central PbPb collisions. The redistribution of the quenched jet energy is studied using the transverse momentum balance of charged tracks projected onto the direction of the leading jet. The momentum balance is recovered by including charged particles at low p_{T} and at large angle with respect to the jet axis. In contrast to pp collisions where the rarer asymmetric dijets are balanced by the hard fragmentation products of third jets, a large fraction of the PbPb momentum balance is carried by low momentum particles at large angular distance to the jet axis.

The measurements presented in these proceedings represent the beginning of a new era in jet quenching studies, relying on the unambiguous identification of both partners in copious, asymmetric dijets. Future studies will include more detailed studies of the fragmentation functions and the flavor-dependence of jet quenching (e.g. via gamma-jet correlations, multi-jet events, and heavy-flavor-tagged jets). Together with future studies, these first measurements will put more powerful, quantitative constraints on the transport properties of hot, dense QCD matter through comparison to theoretical models.

References

[1] **STAR** Collaboration, J. Adams et al., "Evidence from d+Au measurements for final state suppression of high p_T hadrons in Au+Au collisions at RHIC", *Phys. Rev. Lett.* **91** (2003) 072304, arXiv:nucl-ex/0306024. doi:10.1103/PhysRevLett.91.072304.

[2] **STAR** Collaboration, S. Salur, "First Direct Measurement of Jets in $\sqrt{s_{\mathrm{NN}}} = 200$ GeV Heavy Ion Collisions by STAR", *Eur. Phys. J.* **C61** (2009) 761–767, arXiv:0809.1609. doi:10.1140/epjc/s10052-009-0880-y.

[3] **STAR** Collaboration, J. Putschke, "First fragmentation function measurements from full jet reconstruction in heavy-ion collisions at $\sqrt{s_{\mathrm{NN}}} = 200$ GeV by STAR", *Eur. Phys. J.* **C61** (2009) 629–635, arXiv:0809.1419. doi:10.1140/epjc/s10052-009-0904-7.

[4] **CMS** Collaboration, S. Chatrchyan et al., "Observation and studies of jet quenching in PbPb collisions at $\sqrt{s_{\mathrm{NN}}} = 2.76$ TeV", arXiv:1102.1957.

[5] **ATLAS** Collaboration, G. Aad et al., "Observation of a Centrality-Dependent Dijet Asymmetry in Lead-Lead Collisions at $\sqrt{s_{\mathrm{NN}}} = 2.76$ TeV with the ATLAS Detector at the LHC", *Phys. Rev. Lett.* **105** (2010) 252303, arXiv:1011.6182.

[6] **CMS** Collaboration, "The CMS experiment at the CERN LHC", *JINST* **3** (2008) S08004. doi:10.1088/1748-0221/3/08/S08004.

[7] O. Kodolova, I. Vardanian, A. Nikitenko et al., "The performance of the jet identification and reconstruction in heavy ions collisions with CMS detector", *Eur. Phys. J.* **C50** (2007) 117. doi:10.1140/epjc/s10052-007-0223-9.

[8] **CMS** Collaboration, CMS Collaboration, "Determination of the Jet Energy Scale in CMS with pp Collisions at $\sqrt{s} = 7$ TeV", *CMS Physics Analysis Summary* **CMS-PAS-JME-10-010** (2010).

[9] T. Sjöstrand, S. Mrenna, and P. Skands, "PYTHIA 6.4 Physics and Manual", *JHEP* **05** (2006) 026 (tune D6T with PDFs CTEQ6L1 used for 2.76 TeV, tune Z2 for pp 7 TeV), arXiv:hep-ph/0603175.

[10] I. P. Lokhtin and A. M. Snigirev, "A model of jet quenching in ultrarelativistic heavy ion collisions and high-p$_T$ hadron spectra at RHIC", *Eur. Phys. J.* **C45** (2006) 211, arXiv:hep-ph/0506189. doi:10.1140/epjc/s2005-02426-3.

[11] M. Cacciari, G. P. Salam, and G. Soyez, "Fluctuations and asymmetric jet events in PbPb collisions at the LHC", arXiv:1101.2878.